The LiDAR-side of Headwater Streams Mapping Channel Networks with High-resolution Topographic Data

L. Allan James
Kirsten J. Hunt

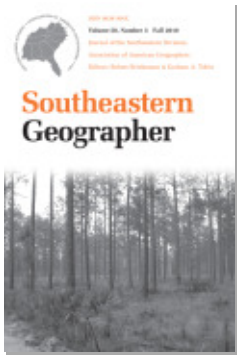

Southeastern Geographer, Volume 50, Number 4, Winter 2010,
pp. 523-539 (Article)

Published by The University of North Carolina Press

The LiDAR-side of Headwater Streams

Mapping Channel Networks with High-resolution Topographic Data

L. ALLAN JAMES
University of South Carolina

KIRSTEN J. HUNT
University of South Carolina

Automated channel headwater mapping methods are reviewed and three methods are used to map a small watershed in the South Carolina upper Piedmont based on high-resolution LiDAR data. First, channels were mapped manually using crenulations on 0.6-m contours generated from the LiDAR data. Field verifications indicate the LiDAR-generated contour map is far superior to the 1:24,000 scale topographic quadrangle and the resulting network map is treated as the reference for assessing network simulations. Second, channel networks were generated using standard flow accumulation methods with three critical area thresholds representing drainage areas of 480, 800, and 1600 m². Third, channel networks were generated using a slope-area product proportional to stream power ($\Omega_{i,j} \propto \mathbf{A}_{i,j}\ \mathbf{S}_{i,j}$). This multivariate method that includes hill-slope gradients improves the identification of small upland channels in steep terrain but may also introduce spurious gully sidewall channels. While all of the methods are capable of simulating fairly accurate channel networks with an appropriate drainage density, errors of omission and commission are greater with the conventional accumulation method and have an association with slope.

Los métodos automáticos para cartografiar canales principales son revisados y tres métodos se utilizan para cartografiar una pequeña cuenca en la altura de la Piedmont de Carolina del Sur basados en datos de alta resolución de LiDAR. En primer lugar, los canales fueron cartografiados manualmente utilizando crenulaciones a 0.6-m en contornos generados a través de los datos de LiDAR. Investigaciones en el campo indican que los mapas de contorno generados con LiDAR son superiores a los cuadrángulos topográficos a escala 1:24,000 y que el mapa de redes resultante es utilizado como referencia para evaluar las simulaciones de red. En segundo lugar, las redes de canales fueron generadas utilizando métodos de acumulación de flujo estándar con tres umbrales de áreas críticas representando áreas de drenaje de 480,800 y 1600 m². En tercer lugar, las redes de canales fueron generadas utilizando un producto de área con pendiente proporcional a la fuerza de la corriente ($\Omega_{i,j} \propto \mathbf{A}_{i,j}\ \mathbf{S}_{i,j}$). Este método de múltiples variable que incluye gradientes de colina-pendiente mejora la identificación de pequeños canales en tierras altas en terreno escarpado, pero puede también reflejar falsos barrancos laterales en los canales. Aunque todos los métodos son capaces de simular de forma certera las redes de canales con una densidad de drenaje apropiada, los errores por omisiones son mayores con el método de acumulación convencional y tiene una asociación con las pendientes.

SOUTHEASTERN GEOGRAPHER, 50(4) 2010: pp. 523–539

KEY WORDS: headwater streams, channel network simulations, small watersheds, Piedmont hydrology

INTRODUCTION

Small watersheds with first- and second-order streams dominate the Earth's land surface. They comprise up to 75 percent of the total length of streams in the United States, yet little is known about where they exist (Leopold et al. 1964; Heine et al. 2004; Somerville and Pruitt 2004; Nadeau and Rains 2007; Fritz et al. 2008). Existing maps of channel networks, drainage divides, and slope configurations are often inaccurate for small watersheds owing to coverage by thick vegetative canopy and coarse resolutions of elevation data. Small watersheds in the humid Southeast tend to be heavily forested, so first- and second-order stream channels are largely obscured by vegetative canopy. Regulatory needs are driving efforts to develop protocols for the field identification and mapping of headwater channels (Gregory et al. 2002; Fritz et al. 2006; NC Division Water Quality 2009). These efforts are concentrating on perennial and intermittent streams, but ephemeral streams and gullies can be equally important in delivering water, sediment, and nutrients downstream in times of flood. Field mapping is generally too expensive for comprehensive county or state-wide mapping projects, but it provides an empirical basis for calibrating other channel network mapping methods based on remote sensing data and modeling.

Field mapping protocols distinguish between perennial and intermittent channels based on biological, hydrological, and morphological criteria. With the exception of the main branch channel at the base of the watershed, which may be intermittent, most of the channels mapped in this paper are ephemeral streams in a deep, well-developed gully system under a mixed forest. Cross-sections of these gullies vary from V-shaped to trapezoidal and range from 0.6 to 6 m deep (Figure 1). They have a pronounced geomorphic expression in the form of banks or sidewalls and important hydrologic consequences, as they result in concentrated flows (as opposed to sheet or shallow subsurface flows) during storm events.

Traditional photogrammetric methods based on aerial photographs are not accurate with regards to the locations of channels and gullies under forest canopy, so drainage densities and morphologies of hillslope features are largely conjectural on modern maps and models (Heine et al. 2004). The lack of elevation data or maps that accurately show locations and densities of channels is a serious limitation to simulating hydrologic responses to storm events. Standard 1:24,000 USGS topographic quadrangles often do not include blue lines or topographic expressions of channels. For example, the map for the small watershed used in this study has limited evidence of channels that are known to exist (Figure 2). Accurate modeling of the production of runoff, sediment, and nutrients in small watersheds ultimately requires physically based or rule-based, spatially distributed models with precise information about slopes and the location and density of channels and gullies.

Airborne laser scanning using Light Detection and Ranging (LiDAR) provides high-resolution elevation data. Although point densities are lower under forest can-

Figure 1. View up ephemeral headwater channel (gully) in study watershed. Photo February 19, 2005.

opy, the data can be used to accurately map channel networks in the Southern Piedmont (James et al. 2007). Several studies have concluded that LiDAR derived DEMs have suitable horizontal and vertical resolutions for mapping channels and surface water flows (Lane et al. 2003; Casas et al. 2006; James et al. 2007; Jones et al. 2008; Perroy et al. in press). The growing availability of high-resolution topographic data from airborne LiDAR will enable a new generation of headwater channel mapping on a nationwide basis. The extent of this mapping will require automated network analysis. Previous work in this area documented the ability of LiDAR data to detect and map channel networks and gullies under forest canopy in small Southeastern watersheds of the South Carolina Piedmont and evaluated the accuracy of channel network maps (James et al. 2007). This paper presents and examines a multivariate stream-power method of automated channel delineation based on the inclusion of hillslope gradients.

Standard methods of drainage network mapping have been developed based on the use of digital elevation models (DEM). The resolution and accuracy of the DEM used is important to the accuracy of the resulting channel network maps, which can be substantially different than ground truth (Walker and Willgoose 1999). Accuracies of hydrologic features have been shown to be sensitive to DEM horizontal resolutions (Wolock and Price 1994). At finer DEM grid-cell sizes, geomorphic features are more accurately depicted, al-

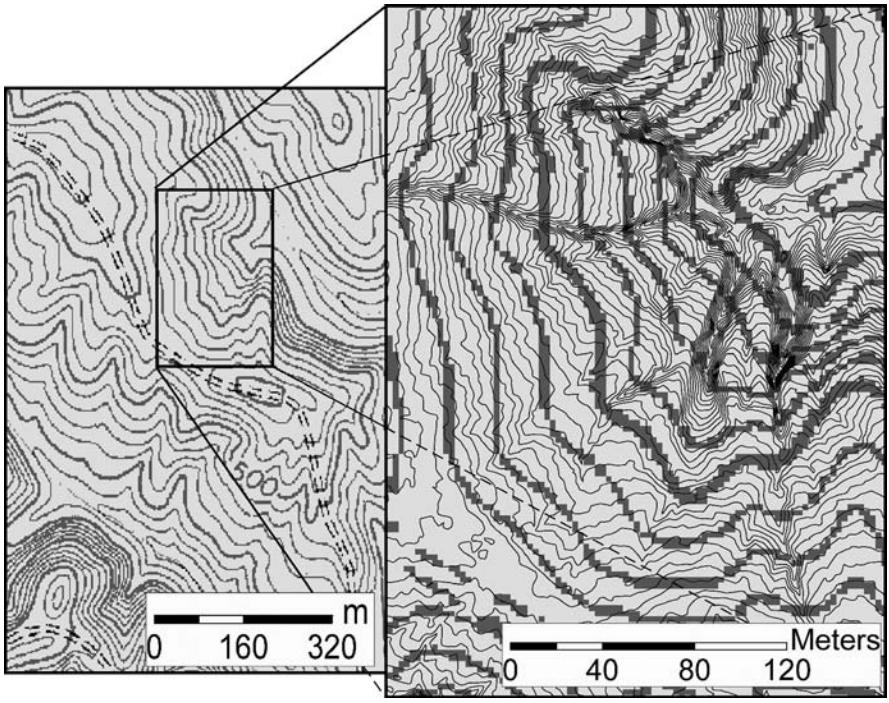

Figure 2. Contour maps of watershed near Macedonia Lake, South Carolina. Left map is an excerpt from USGS 1:24,000 quadrangle. At right is a blow-up of the map with LiDAR 0.6-m contours overlain. No blue lines are shown in this watershed on the USGS map, yet gullies depicted clearly by LiDAR contours correspond with deep, field-verified ephemeral or intermittent channels.

though the minimum cell size is constrained by the quality of the original survey data (Zhang and Montgomery 1994). Accuracies of standard DEMs are also limited by vertical resolutions; e.g., ±7 m in the early USGS 30 m DEMs (Kenward et al. 2000). Many geomorphic environments, such as floodplains, deltas, wetlands, and estuaries, are characterized by low-relief, so the use of standard DEMs for mapping channels is problematic. Interpolation methods used in developing DEMs may also affect their accuracy (Aguilar et al. 2005), and these errors should be considered and reported.

AVAILABILITY OF HIGH-RESOLUTION TOPOGRAPHIC DATA

The effectiveness of methods for processing DEMs will benefit from on-going efforts to develop high-resolution data (e.g. LiDAR-derived DEMs) in the USA. It is widely recognized that a national LiDAR dataset will benefit many state and federal agencies such as the Federal Emergency Management Agency's (FEMA) flood map modernization effort (NRC 2007). A recent National Research Council study recommended that FEMA increase collaboration with federal, state, and local government

agencies in the acquisition of LiDAR-derived topographic data throughout the nation (NRC 2009). The *National LiDAR Mapping Initiative,* also known as the *Elevation for the Nation* (EFTN) program, is an effort to collect accurate, seamless, high-resolution elevation data for the 50 states through implementation of medium-altitude, advanced technology. The *American Recovery and Reinvestment Act* of 2009, aka the economic stimulus plan, included funding for the EFTN program to parallel the Imagery for the Nation (IFTN) program. Advances in LiDAR technology have reduced costs of acquisition, increased point densities and accuracies, and improved post-processing accuracies, thus increasing the practicality of a national digital mapping program based on LiDAR technology. Updating of the National Elevation Dataset (NED) has been employing LiDAR data since 2002 and making it available on the internet. The NED is the elevation layer of the National Map, a seamless dataset in the public domain. NED provides raster elevation data at three scales ranging from 1 arc second (~30 m) down to 1/9 arc-second (~3 m) data that are derived from bare earth LiDAR elevation data. While the NED is dominated by older data, it is updated on a two-month cycle to add improved elevation data as they become available, and the coverage of 3-m LiDAR-derived data in the public domain is rapidly growing. As with the entire National Map, data from the NED can be accessed through the *Seamless Data Distribution System* (SDDS).

The U.S. Geological Survey is the designated lead Federal agency for collecting and distributing digital cartographic data. The USGS incorporates DEM data into the *National Digital Cartographic Data Base* (NDCDB) according to specific standards (USGS 2000) designed to ensure quality and compatibility between products. Modern LiDAR systems are capable of producing elevation data exceeding the resolutions of the NED 1/9 arc-second (~3 m) data, and the spatial resolutions and accuracies of LiDAR-derived bare Earth DEMs continue to improve. Moreover, additional applications of LiDAR data are promising and new products can be anticipated. For example, advances in the analysis of LiDAR intensity values improve identifications of soil, vegetation, land-use and land-cover, and bare Earth from LiDAR imagery (Yoon et al. 2008; Cheng and Glenn 2009). This paper utilizes DEMs derived from standard LiDAR bare-earth products processed by Ayers and Associates.

HEADWATER STREAM MAPPING CONCEPTS

Traditional methods for automated drainage network mapping and stream ordering based on flow-accumulation grids derived from DEMs have been around for more than twenty years (Jenson and Domingue 1988; Lanfear 1990; Martz and Garbrecht 1993). These methods are accurate for mapping locations of fourth-order and higher streams in large basins if suitable elevation data are available. For small watersheds in humid regions where forest canopies obscure the ground surface, however, conventional topographic data lack the spatial resolution and accuracy for mapping first- and second-order streams, so drainage densities cannot be accurately determined. Although the quality of LiDAR-derived topography is decreased by vegetation canopy, some proportion of the pulses often penetrates through the canopy to the ground and is returned to the

sensor. Thus, LiDAR data have the capability of providing maps of channel networks for small watersheds under forest canopy in the southern Piedmont at unprecedented accuracies (James et al. 2007). These channel networks have much higher drainage densities than previous maps, indicating that the delivery of water and sediment is substantially more efficient than would be expected based on existing maps of channel networks or from networks derived from contour crenulations on 1:24,000 maps. Yet, channel network maps resulting from standard flow accumulation methods alone have errors of omission and commission indicating that standard methods can be improved upon. First, conditions for channel initiation have conventionally been based solely on flow accumulation; i.e., channels begin above a specific number of cells contributing flow from upslope. The critical area threshold for channel initiation must be specified. This should be done with field calibrations, but LiDAR data can greatly improve constraints on the extent of small channels to test critical area assumptions using remote sensing methods. Second, channel initiation on hillslopes is not simply a function of runoff (as measured by drainage area or flow accumulation). Channel initiation results also from topographic factors including slope gradients, plan and slope curvature (Tarboton 1991; Heine et al. 2004), and erodibility factors such as land-use/land-cover, soil type, and vegetation cover. Thus, locating headwater channels is a multivariate problem and univariate mapping solutions, such as the threshold accumulation method, should be considered as only a first approximation.

Headwater channel locations are likely to be strongly influenced by stream power or power functions of discharge and slope (Nearing et al. 1997; Istanbulluoglu et al. 2003). Given that stream power is proportional to the product of discharge and slope ($\Omega \propto QS$), and assuming that discharge is approximately proportional to drainage area ($Q \propto A$), then values of the slope-area product grid should be proportional to stream power ($\Omega \propto AS$). One simple modification of flow accumulation models, therefore, is to calculate the simple product of the flow accumulation and slope grids:

$$\Omega_{i,j} \propto \mathbf{A}_{i,j}\, \mathbf{S}_{i,j} \tag{1}$$

where i and j are grid cell coordinates in the DEM raster. This method can be used to map headwater channels by setting a critical stream power threshold (Ω_C). Similarly, some studies of hillslope channel initiation suggest that the critical threshold for initiation (A_{cr}) can be expressed as a simple function of the product of accumulation area and a power of slope (Istanbulluoglu et al. 2002):

$$A_{cr} = b\, AS^{\beta} \tag{2}$$

where b and β are empirically derived coefficients. Finally, the critical area of stream-head locations has been predicted based on a slope-power relationship expressed in terms of the slope tangent (Montgomery and Foufoula-Georgiou 1993; Heine et al. 2004):

$$A_{cr} = c\, (\tan\theta)^{\gamma} \tag{3}$$

where A_{cr} is the critical area of channel initiation, θ is slope angle (degrees), and c and γ are empirical power-relationship coefficients. Coefficients for Equation 3 can be established empirically using statistical

regression of log A_{cr} on log tanθ (Heine et al. 2004). The approaches indicated by Equations 2 and 3 both assume that channel initiation is governed by a single accumulation threshold (critical drainage area) and focus on the identification of this critical area. A true multivariate approach, however, acknowledges that channel initiation is governed by other factors so that the drainage areas of various channel heads may vary. This paper presents a simple step in this direction by adding slope to the analysis of drainage areas.

Table 1. Methods for automated mapping of headwater channels using stream power.

1. Generate reference channel network using contour crenulation method on contour maps created from LiDAR DEM.
2. Generate flow direction and accumulation grids using DEM created from LiDAR data.
3. Compute area grid ($\mathbf{A}_{i,j}$) from accumulation grid as product of accumulation values and grid-cell area; e.g., 3x3-m grid cell is 9 m^2, so cell with an accumulation of 100 cells has 900 m^2 contributing area .
4. Create slope grid ($\mathbf{S}_{i,j}$) from LiDAR DEM. Convert to percent slope to enable use of integer values in grid.
5. Compute stream-power (Ω) grid as product of area and slope grids: $\Omega_{i,j} \propto \mathbf{A}_{i,j}\, \mathbf{S}_{i,j}$.
6. Identify channels on $\Omega_{i,j}$: Set critical threshold of stream power (Ω_C) and assign all $\Omega_{i,j} \geq \Omega_C$ to 1 and all other cells to 0.
7. Compare simulated channel network drainage density and topology with reference network. If too many channels in simulation, increase Ω_C and repeat step 4. If too few, decrease Ω_C.

METHODS

This study is focused on a small watershed (7 ha) in the South Carolina upper Piedmont (Figure 3) that experienced severe erosion during the early twentieth century owing to land clearance for agriculture. As with many watersheds in the region, agriculture declined substantially in the early 20th century, and much land cover reverted to mixed hardwood-coniferous forest with a moderately dense canopy. The LiDAR data used in this study were collected by Ayers and Associates with a fixed-wing aircraft in April, 2004 for the U.S. Forest Service (USFS), Enoree Ranger District. The April flight optimizes for leaf-off conditions of the hardwoods, although coniferous canopy remained present. Bare-Earth filtering was done by Ayers and Associates who provided the USFS with X, Y, Z values in state plane coordinates, which were converted to shapefiles and reprojected into UTM coordinates (James et al. 2007). No point cloud data were available for analysis in this study. The resulting bare-Earth point densities were 1275 points/ha or an average point spacing on the order of 3.0 m, although the point density was not uniform. These point data were used to generate a TIN, 4x4-m gridded DEM, 4x4-m slope grid, and a contour map at 0.6 m intervals.

The steps used to simulate and evaluate channel networks are outlined in the Table 1. A reference channel network map was manually created using the contour crenulation method on the detailed contour map with 0.6 m contour intervals generated from LiDAR DEMs (Figure 4). Many of the crenulated channels were field verified, and some channel locations were manually adjusted based on field

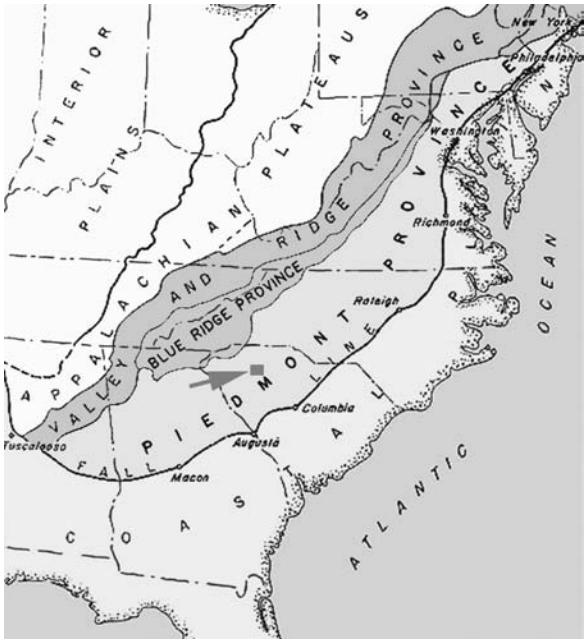

Figure 3. Physiographic map of southeastern USA showing upper Piedmont and South Carolina study area in Union County (small square). Base map from Ireland et al. 1939.

knowledge (James et al. 2007). This channel network map is treated as the reference layer for validations of various automated mapping methods. A slope map was generated from the LiDAR DEM using standard nearest neighbour relationships (Figure 5). In the test watershed, slopes on the map range from zero to 58 percent. These gradients are conservative because these LiDAR data tend to underestimate gully depths and side slopes under the mixed forest canopy (James et al. 2007). The slope map reveals the spatial pattern of relatively low gradients near divides and at the base of the depositional fan near the outlet, with maximum gradients on gully side slopes. Beyond the gullies, the slope map indicates a steep zone in the north end of the watershed and a low-gradient zone in the central west area.

Three simulated channel networks were automatically generated using the standard flow-accumulation method (Jenson and Domingue 1988) with LiDAR-derived DEMs. The standard method identifies channels by creating flow-direction and flow-accumulation grids, comparing grid-cell values in the accumulation grid to a critical threshold of drainage area (accumulation threshold), and assigning all grid cells with values greater than the threshold equal to 1 and lesser grid cell values to 0. The three networks were de-

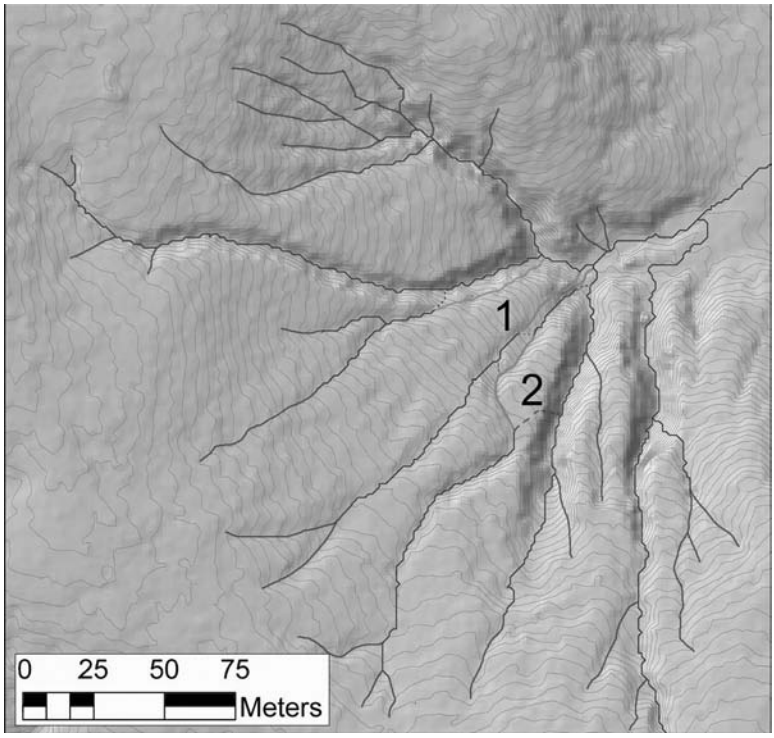

Figure 4. Headwater channels mapped using contour crenulations on a shaded relief base map derived from LiDAR point data. The reference network was manually edited to remove a few errors based on field knowledge. At '1' two pairs of parallel gullies were erroneously merged into single channels by all of the simulations. At '2' all simulations missed the northwest channel and diverted flows eastward into a deep gully. This corrected network was used as the reference to evaluate simulations.

rived from the flow accumulation grid by setting critical accumulation thresholds at 30, 50, and 100 grid cells (critical drainage areas of 480, 800, and 1600 m^2, respectively). These thresholds were selected after trial runs by identifying a threshold value that approximated the drainage density of the reference network and two other thresholds bracketing that value. Another set of three channel networks was mapped by computing slope-area products (SA) from the flow accumulation and slope grid (Equation 1). The three SA threshold were also selected by comparison of drainage densities with the reference network. Channel grid cells were determined by the same threshold method as for the flow accumulation method using values of SA as thresholds to generate a range of drainage densities. One of the three thresholds selected for each model is close to the reference drainage

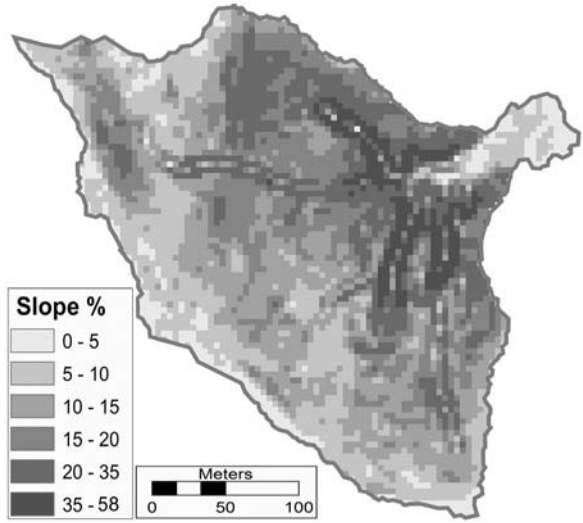

Figure 5. Percent slope grid ($S_{i,j}$) generated from LiDAR DEM. Highest gradients (dark zones) are associated with gully side slopes and with broad areas in north half of watershed.

density which was used as the initial criterion for evaluation. The ultimate success of each model is based on a qualitative assessment of spatial locations of channels within the watershed in comparison with the reference channel network determined by the contour crenulation method with field verification.

All channel grid cells were converted to vectors for mapping and computation of drainage densities (Σchannel length / drainage area). Each network was compared to the reference network generated by contour crenulation methods. In both sets of experiments, three arbitrary threshold values are reported including one with a similar drainage density to the reference channel network. Comparisons were made based on drainage densities, percent accuracies of channel cell identifications, errors of omission and commission, and a visual assessment of channel network topology.

RESULTS

By all of the methods employed, channel networks derived from the LiDAR DEMs are substantially more dense and closer to field observations than channel networks derived from the 1:24,000 map using blue lines or contour-crenulations. No blue lines are mapped in the watershed on the 1:24,000 quadrangle, so the blue-line method failed to identify any of the numerous channels observed in the field (Table 2). The network generated by the contour crenulation method using 1:24,000 quadrangle contours had a drainage density of only 11.6 m km^{-2} compared to 34.5 m km^{-2} for the LiDAR contour-crenulation map used as the ref-

erence. Simulated networks derived by standard flow-accumulation and power methods had a wide range of drainage densities and stream magnitudes that varied with the thresholds used. In general, stream order was far too insensitive to be used to evaluate differences in networks. Conversely, stream magnitudes were far too sensitive to the number of very small tributaries that may be generated by simulations. Drainage density is considered the best single metric for tuning the models, because it provides a quantitative measure of topologic completeness and hydrological response; i.e., network density is strongly related to the efficiency of water and sediment conveyance. Since drainage area is constant, drainage densities are proportional to total channel length for each simulated network. On the basis of drainage densities, a threshold of 30 cells provided the best network by the accumulation method and a threshold of SA=750 provided the best network by the stream power method. Either method could be fine-tuned to drainage density by iterations of threshold values, so other criteria are needed to compare the success between the two methods.

Table 2. Channel network parameters for the Macedonia watershed.

Drainage area: 70,010 m^2.

	Stream Order	Stream Magnitude	Drainage Density (m/km^{-2})
Contour Crenulation (manual interpretations):			
1:24,000 quad	3	5	11.6
Lidar DEM[a]	**4**	**31**	**34.5**
Conventional Accumulation Method:			
Threshold 30	4	31	35.1
Threshold 50	4	19	28.2
Threshold 100	3	13	19.9
Stream Power Method:			
Threshold 250	4	63	46.1
Threshold 500	4	45	32.3
Threshold 750	4	31	26.3

[a]Reference network.

The blue-line method, which uses only streams depicted on 1:24,000 maps, had zero values in all four categories; i.e., there were no blue lines in the study watershed.

An error analysis was conducted by converting the reference network to rasters and using that grid to compute errors for each of the six experiments (Table 3). The error analysis gives the number of cells that are accurately classified as channels or not channels, as well as errors of omission and commission. The Power 500 and 750 networks provided the highest total percentage of grid cells correctly classified ("Accuracy" on Table 3), but the range of values between all six experiments was between 85.1 and 87.1 percent. The small difference reflects that fact that total accuracy is driven by the large number of non-channel cells that are correctly classified in all cases. More sensitive assessments are provided by the percentage of correctly identified channel cells and errors of omission and commission. As might be expected, lower thresholds generate more channels, so they identify higher percentages of channel cells, higher errors of commission, and lower errors of omission (%ch correct, %Ec and %Eo, respectively on Table 3). In general, the power networks identified a larger percentage of channel cells with lower errors of omission than the accumulation networks, but they also committed higher errors of commission.

Table 3. Errors of omission and commission from grid-cell counts using LiDAR contour crenulations network as reference.

Method	Channel	Not channel	Error Classes[a] Ch	H	Eo	Ec	Total Correct	Total Error	Accuracy (%)[b]	%Ch correct[c]	%Ec[c]	%Eo[c]
Crenul.	778	3600					4378					
Accumulation												
30	547	3831	355	3408	423	192	3763	615	86.0	45.6	24.7	54.4
50	440	3938	301	3461	477	139	3762	616	85.9	38.7	17.9	61.3
100	309	4069	247	3538	531	62	3785	593	86.5	31.7	8.0	68.3
Power												
250	724	3654	425	3301	353	299	3726	652	85.1	54.6	38.4	45.4
500	514	3864	361	3447	417	153	3808	570	87.0	46.4	19.7	53.6
750	416	3962	315	3499	463	101	3814	564	87.1	40.5	13.0	59.5

[a]Success/Error Classes

Ch = correctly classified as channel

H = correctly classified as not channel (hill slope)

Eo = incorrectly classified as not channel (error of omission)

Ec = incorrectly classified as a channel (error of commission)

[b]Percent accuracy = number correct / total number cells

[c]%Ch correct, %Ec, and %Eo are percentages of total channel cells correct, errors of commission, and errors of omission, respectively, all calculated as proportions to 778, the total number of channel cells in the reference network.

Visual inspection of the networks is essential to an accurate assessment of the spatial pattern determined by a given method. Cell-by-cell error evaluations often miss important aspects of a quality assessment that may be visually obvious; e.g., distributary channels or channels crossing sub-divides within the watershed. While the best estimate of drainage density was obtained with an accumulation threshold of 480 m^2 (30 cells), several channels in that network extend too far up into the low-gradient convex slopes near the western divide (Figure 6). In this respect, the network generated using a critical area threshold of 800 m^2 (50 cells) in the conventional critical threshold method provided a topologic structure more in keeping with the reference network. The quantitative error data (Table 3), however, indicate that the difference between the two simulated networks is primarily a trade-off between errors of omission and commission. The decrease in errors of commission in shifting from a threshold of 30 to a threshold of 50 was compensated for by an approximately equal increase in errors of omission. Clearly, factors other than drainage area must explain some of the channels in the control group that were omitted in the simulations.

When hillslope gradient is added to network simulations through computation of stream powers the resulting channel

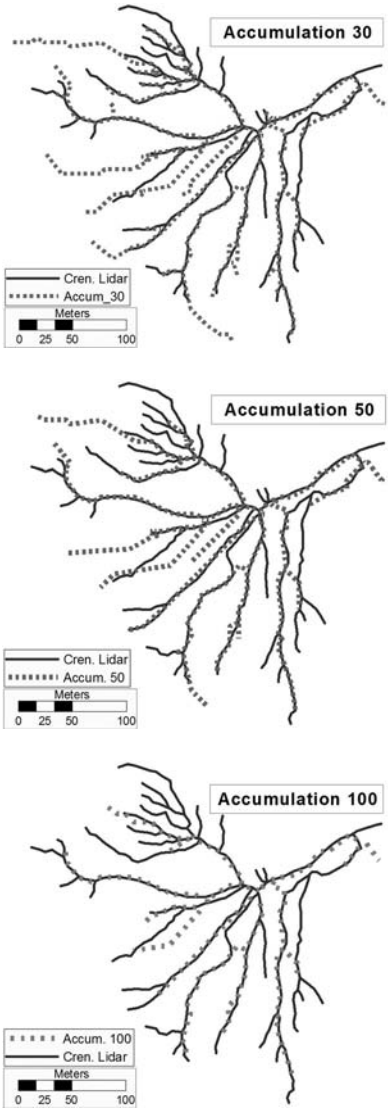

Figure 6. Channel networks derived by the conventional flow accumulation method with various critical area thresholds (A_{cr}). Upper left: A_{cr} = 30 provides drainage density closest to reference network but many locations of channels are incorrect. Upper right: A_{cr} = 50 underestimates drainage density. Lower right: A_{cr} = 100 greatly underestimates drainage density.

maps are improved (Figure 7). The power network generated with a threshold of 500 provides a fairly good topological resemblance to the reference network. Total accuracy is high (87 percent), and errors of omission and commission are moderately low. Most importantly, the high gradient zone in the northern watershed has more channels than the accumulation model, and the low-gradient zone in the west has fewer channels. Both of these features are in accordance with the reference network (Figure 8).

DISCUSSION

The power method appears to have the potential to improve on the conventional accumulation method, especially in areas of variable gradient where the presence or absence of channels may be influenced by shear stresses of flows. This concept and the simple application demonstrated here needs to be tested on more headwater stream and gully systems in a variety of environments to see if it is robust. In all cases of automated channel network mapping, field calibration to determine thresholds and verify model predictions is essential to reliable mapping. Further improvements to simulation methods, such as filtering out short first-order streams, are being explored.

Errors of omission and commission remain substantial in all of the models produced (Table 3), suggesting that a higher order method of hillslope gradients or multivariate approaches could be beneficial. All of the grid-simulated networks reported here rely on the same flow-direction and flow-accumulation grids, and a few topological errors embedded in the flow direction model were promulgated

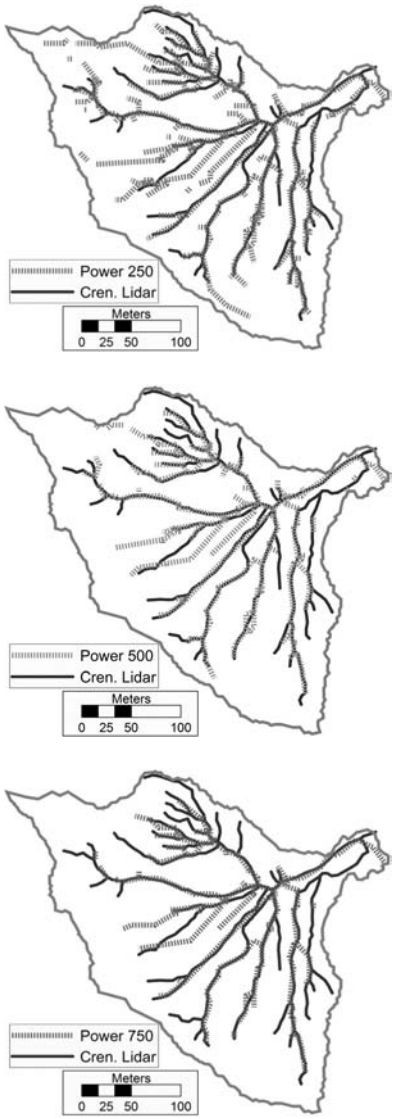

Figure 7. Stream-power networks based on Equation 1 ($\Omega_{i,j} = \mathbf{A}_{i,j}\,\mathbf{S}_{i,j}$). Solid lines show the contour crenulation reference network; dashed lines are simulated networks.

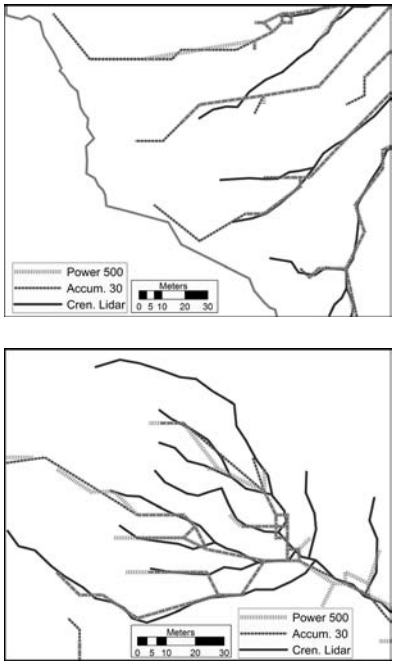

Figure 8. Three stream networks for two selected subbasins. Top: west side of watershed showing low gradient zone where accumulation method extends too far but power method is similar to reference network. Bottom: steep north side of watershed where network generated by accumulation method fails to capture most of the streams in the reference network. The power method produced better results despite errors of omission and commission.

through all subsequent analysis (Figure 4). For example, this watershed has closely-spaced parallel channels in places that the 4-m LiDAR DEM was not capable of discriminating (James et al. 2007). While the LiDAR DEMs provide a substantial improvement over earlier topographic data sets, errors in the flow direction model represent pure error in the analysis that should be corrected in an early phase of the analysis through field mapping and hydroburning techniques. In addition to errors inherent to the DEMs, some variability in the reference channel networks is likely to be the result of multivariate complexity that cannot be completely explained by simple functions of drainage area or slope. Factors such as soil type, vegetation, or incipient conditions (e.g., rills forming in plowed furrows 50 years ago) may explain some channels that won't appear on simulations.

CONCLUSION

Topographic information provided by LiDAR bare Earth data produce elevation models that are substantial improvements over standard DEMs. Contour maps derived from these DEMs allow delineation of headwater channel and gully networks by conventional contour crenulation methods that are good first approximations of channel networks observed in the field. Network maps derived from the LiDAR DEMs were generally of good quality. Using the crenulation map to calibrate thresholds for accumulation and power thresholds is helpful but field verification of maps is essential. Standard accumulation methods produced reasonable results, but inclusion of the slope-area product appears to provide additional channel predictive capabilities. In areas of highly variable hillslope gradients, the power method may provide a simple means of discriminating between slopes with equal accumulation areas that are channelized and those that have no channels.

REFERENCES

Aguilar, F.J., Aguera, F., Aguilar, M.A., and Carvajal, F. 2005. Effects of terrain morphology, sampling density, and interpolation methods on grid DEM accuracy. *Photogrammetric Engineering and Remote Sensing* 71(7):805–816.

Casas, A., Benito, G., Thorndycraft, V. R., and Rico, M. 2006. The topographic data source of digital terrain models as a key element in the accuracy of hydraulic flood modeling. *Earth Surface Processes and Landforms* 31:444–456.

Cheng, W., and Glenn, N.F. 2009. Integrating LiDAR intensity and elevation data for terrain characterization in a forested area. *Geoscience and Remote Sensing Letters*, IEEE 6(3):463–466.

Colson, T.P., Gregory, J.D., Mitasova, H., and Nelson, S.A.C. 2006. Comparison of stream extraction models using Lidar DEMs. In *Geographic Information Systems and Water Resources*, IV AWRA, Spring Specialty Conference, Houston, Texas, May 8–10, 2006.

Fritz, K.M., Johnson, B.R., and Walters, D.M. 2006. *Field Operations Manual for Assessing the Hydrologic Permanence and Ecological Condition of Headwater Streams*. EPA/600/R-06/126. U.S. Environmental Protection Agency, Office of Research and Development, Washington DC.

Fritz, K.M., Johnson, B.R., and Walters, D.M. 2008. Physical indicators of hydrologic permanence in forested headwater streams.

Journal of the North American Benthological Society 27(3):690–704.

Garbrecht, J., and Martz, L. 1993. Case application of the automated extraction of drainage network and subwatershed characteristics from digital elevation models by DEDNM. In Lanfears, K. and Harlin, J. (eds.), *Geographic Information Systems and Water Resources,* American Water Resources Association, p. 221–229.

Gregory, J.D., Smith, S.D., Fleek, E., Penrose, D. 2002. What is a stream? *Proceedings Water Environment Federation*, Watershed 2002, p. 374–398.

Heine, R.A., Lant, C.L., and Sengupta, R.R. 2004. Development and comparison of approaches for automated mapping of stream channel networks. *Annals of the Association of American Geographers* 94(3):477–490.

Istanbulluoglu, E., Tarboton, D.G., Pack, R.T., and Luce, C. 2002. A probabilistic approach for channel initiation. *Water Resources Research* 38(12), 1325, doi:10.1029/2001WR000782.

——, Tarboton, D.G., Pack, R.T., and Luce, C. 2003. A sediment transport model for incision of gullies on steep topography. *Water Resources Research* 39(4), 1103, doi:10.1029/2002WR001467, 2003.

James, L.A., Watson, D.G., Hansen, W.F. 2007. Using Lidar to map gullies and headwater streams under forest canopy: South Carolina, USA. *Catena* 71:132–144.

Jenson, S. K., and Domingue, J. O. 1988. Extracting topographic structure from digital elevation data for geographic information system analysis. *Photogrammetric Engineering and Remote Sensing* 54(11):1593–1600.

Jones, K. L., Poole, G.C., O'Daniel, S.J., Mertes, L.A.K., Stanford, J.A. 2008. Surface hydrology of low-relief landscapes: Assessing surface water flow impedance using LIDAR-derived digital elevation models. *Remote Sensing of Environment* 112:4148–4158.

Kenward, T., Lettenmaier, D.P., Wood, E.F., and Fielding, E. 2000. Effects of digital elevation model accuracy on hydrologic predictions. *Remote Sensing of Environment* 74(3):432.

Lane, S.N., James, T.D., Pritchard, H., and Saunders, M. 2003. Photogrammetric and laser altimetric reconstruction of water levels for extreme flood event analysis. *Photogrammetric Record* 18:293–307.

Lanfear, K.J. 1990. A fast algorithm for automatically computing Strahler stream order. *Water Resources Bulletin* 26(6):977–979.

Leopold, L.B., Wolman, M.G., and Miller, J.P. 1964. *Fluvial Processes in Geomorphology*. Dover Publications, N.Y.

Nadeau, T.L., and Rains, M.C. 2007. Hydrological connectivity between headwater streams and downstream waters: How science can inform policy. *Journal of the American Water Resources Association* 43:118–133.

National Elevation Dataset (NED). Accessed 21 August 2009 at http://ned.usgs.gov/.

National Research Council Committee on Floodplain Mapping Technologies. 2007. *Elevation Data for Floodplain Mapping,* 168pp.

——. Committee on FEMA Flood Maps. 2009. *Mapping the Zone: Improving Flood Map Accuracy*, 136pp.

North Carolina Division of Water Quality. 2009. *Methodology for Identification of Intermittent and Perennial Streams and their Origins, Version 4.0*. NC Dept. Environment and Natural Resources, Division of Water Quality. Raleigh, NC.

Perroy, R. L., Bookhagen, B., Asner, G.P.,

Chadwick, O.A. 2010. Comparison of gully erosion estimates using airborne and ground-based LiDAR on Santa Cruz Island, California. *Geomorphology*, in press.

Somerville, D.E., and Pruitt, B.A. 2004. *Draft Physical Stream Assessment: A Review of Selected Protocols*. Prepared for the U.S. Environmental Protection Agency, Office of Wetlands, Oceans, and Watersheds, Wetlands Division (Order No. 3W-0503-NATX). EPA, Wash., D.C.

U.S. Geological Survey National Mapping Division. 2000. *Standards for Digital Elevation Models. National Mapping Program Technical Instructions*. Accessed 23 August 2009 at http://rockyweb.cr.usgs.gov/ nmpstds/acrodocs/dem/1DEM0897.PDF.

Walker, J., and Willgoose, G. 1999. On the effect of digital elevation model accuracy on hydrology and geomorphology. *Water Resources Research* 35(7):2259–2268.

Wolock, D.M., and Price, C.V. 1994. Effects of digital elevation model map scale and data resolution on a topography-based watershed model. *Water Resources Research* 30:3041–3052.

Yoon, J.S., Shin, J.I., and Lee, K.S. 2008. Land cover characteristics of airborne LiDAR intensity data: A case study. *Geoscience and Remote Sensing Letters*, IEEE 5(4):8012–805.

Zhang, W., and Montgomery, D.R. 1994. Digital elevation model grid size, landscape representation, and hydrologic simulations. *Water Resources Research* 30(4):1019–1028.

L. ALLAN JAMES is a Professor in the Department of Geography at the University of South Carolina, Columbia, SC 29208. Email: *ajames@sc.edu*. His research interests include river and watershed science, fluvial geomorphology, human-environment interactions, water resources, and hydrogeomorphic applications of GI Science.

KIRSTEN J. HUNT is a second-year Ph.D. student in the Department of Geography at the University of South Carolina, Columbia, SC 29208. Email: *huntkj@email.sc.edu*. Her research interests include fluvial geomorphology, remote sensing, and GI Science.